

Harmonic balance method with alternating frequency/time domain technique for nonlinear dynamical system with fractional exponential*

Zhi-yong ZHANG (张智勇), Yu-shu CHEN (陈予恕)

(School of Astronautics, Harbin Institute of Technology, Harbin 150001, P. R. China)

Abstract Comparisons of the common methods for obtaining the periodic responses show that the harmonic balance method with alternating frequency/time (HB-AFT) domain technique has some advantages in dealing with nonlinear problems of fractional exponential models. By the HB-AFT method, a rigid rotor supported by ball bearings with nonlinearity of Hertz contact and ball passage vibrations is considered. With the aid of the Floquet theory, the movement characteristics of interval stability are deeply studied. Besides, a simple strategy to determine the monodromy matrix is proposed for the stability analysis.

Key words fractional exponential nonlinearity, harmonic balance method with alternating frequency/time (HB-AFT) domain technique, global response, stability

Chinese Library Classification O322

2010 Mathematics Subject Classification 70K50

1 Introduction

All periodic motion of linear dissipation system is stable. However, some periodic motion for nonlinear dissipation system is unstable. There may be many different types of motion, such as super-harmonic, sub-harmonic, and chaotic vibrations. The analysis of motion types and stable regions of engineering system has important significance. It is common to use the fractional exponential model to describe impact and contact problems in engineering^[1]. However, the dynamic response of this model is difficult for theoretical analysis^[2]. Therefore, it is necessary to find an effective method for these problems.

A semi-analytical method of implicit harmonic balance analysis named the harmonic balance method with alternating frequency/time (HB-AFT) domain technique was first proposed by Yamauchi in 1983^[3]. Kim and Noah^[4–6] developed this method to a complete solution strategy for the periodic response of dynamic systems. The homotopy continuation scheme together with the HB-AFT method was provided to compute hysteresis response by Groll and Ewins^[7]. Tiwari and Gupta^[8] first used the HB-AFT method to the bearing-rotor systems considering ball passage vibrations to validate the steady response obtained by numerical integration. Villa et al.^[9] used a whole frequency domain method based on the HB-AFT and a perturbation method to study the response characteristic in a flexible ball bearings-rotor system. However, it should be noted that this whole frequency domain method in Ref. [9] cannot generate the bifurcation mechanism of instability locations.

* Received Mar. 8, 2013 / Revised Jun. 13, 2013

Project supported by the National Natural Science Foundation of China (No. 10632040)

Corresponding author Zhi-yong ZHANG, Ph. D., E-mail: zhiyongzhang@126.com

In this paper, we present the advantage of the HB-AFT method for fractional exponential problems. The global response of a two degree-of-freedom ball bearing-rotor structure is deeply analyzed by the HB-AFT approach combined with the Floquet theory, and for the first time, we attempt to estimate the dangerous unstable ranges of with this system via the above schemes.

2 Comparison of solving methods

There are many numerical and analytical methods for the study of steady state of differential dynamical systems. Usually, we take the problems as initial value problems of ordinary differential equations and solve the systems with numerical integration. The Runge-Kutta (R-K) method is among the most popular classes of formulas for the numerical integration of initial value problems. Unlike the multi-step methods, it is a one-step method, and one can change the step size of integration as often and by as much as required. Therefore, it is usually effective for stiff equations^[10], although a higher-order R-K method requires more function evaluations per integration step. However, the R-K method only can obtain asymptotic steady-state response, and it may take a long time of integration for a system with a smaller damping^[4]. Furthermore, the initial value problems cannot be used to obtain the unstable periodic response^[11]. This brings difficulties for the analysis of the bifurcation characteristics of periodic motion. The resolution of the responses of dynamic systems can also be converted to a boundary-value problem. Then, one can use the shooting method or finite-difference schemes to solve the problem. The shooting algorithm and its modified methods^[12-14] are widely used in engineering^[15-16]. However, the initial value and the integration step-size have a great effect on the convergence and the convergent speed^[17-18]. Moreover, a heavy computation is often needed, especially when the period of the system's response is very large, e.g., in some cases dealing with multiple-input frequencies^[19].

In terms of analytical methods, the common methods, such as the small parameter method, the average method, and the multi-scale method, are effective for characteristics investigation of weakly nonlinear systems. When dealing with strong nonlinearity, the harmonic balance method is usually used. However, the calculation accuracy is hard to ensure^[17,20].

All methods developing from the classic harmonic balance (HB) method, e.g., the incremental harmonic balance (IHB) method, the HB-AFT method, and the generalized harmonic balance (GHB) method, can provide periodic solutions in form of trigonometric series. The IHB method was first proposed by Lau and Cheung in 1981^[21]. The basic idea of the approach is as follows: first, suppose the solution to the system is harmonic; then, deduce the incremental equation of the harmonic coefficients; finally, obtain the result by the iteration of the incremental equation. The IHB method is very effective in analyzing the periodic behaviors of smooth dynamics^[22], and it can be used to deal with piecewise-linear problems^[23-24]. However, because of the incremental equation of the system usually obtained by Taylor series expansion^[25], this method is difficult to deal with nonlinear systems with piecewise discontinuity from the mathematical definition^[26-27]. In recent years, the GHB method has been developed by Luo^[28-29]. The authors, by the averaging idea, set the solution to the system with harmonic terms and supposed that the coefficients of these terms vary slowly with time. The algebraic equations of the coefficients were obtained by harmonic balance process, and the solutions were derived by any iteration strategy. These solutions and their bifurcation behaviors could be determined from the analysis of the stability about the equilibrium point by a perturbation of the harmonic terms. The GHB method provides an analysis tool for chaos systems^[28]. However, because of the average idea^[30], the nonlinear function should be integrated in the process of computation, which makes it a challenge for the problem with complicated integration.

For nonlinear systems, the main idea of the HB-AFT is as follows:

$$\ddot{x}(t) = f(\ddot{x}, \dot{x}, x, t). \quad (1)$$

To analyze its periodic solution property, it is assumed that $x(t) = x(t+T)$, where T represents

the period of $x(t)$. Then, $x(t)$ and $f(\cdot)$ can be written as two groups of Fourier series expansions with the same orthogonal basis. According to Eq. (1), one can get an implicitly nonlinear algebraic relationship between the harmonic coefficients of $x(t)$ and $f(\cdot)$. With the aid of the discrete Fourier transform (DFT) and the inverse discrete Fourier transform (IDFT), the information used to iterate the implicitly algebraic can be obtained. Thus, it can be seen that the HB-AFT method is different from the IHB method and the GHB method. It establishes relationships of each order harmonic term directly from the discrete time frequency features, and there is little integration and analytical work required during the solving process of the HB-AFT method. Thus, this method can be considered to be more versatile for the strong nonlinear problems with piecewise fractional exponential.

3 Model and methods

3.1 Bearing-rotor model

For the ball bearing, as shown in Fig. 1, when only consider the effects of Hertz contact and ball passage vibrations on the bearing-rotor system, the classical 2-DOF model of ball bearing is enough for the qualitative analysis^[31]. Thus, the constitutive equation of a rigid rotor with the ball bearing is expressed as

$$m \begin{bmatrix} \ddot{x} \\ \ddot{y} \end{bmatrix} + C \begin{bmatrix} \dot{x} \\ \dot{y} \end{bmatrix} + C_b \sum_{i=1}^{N_b} G(\delta_i)^{1.5} \begin{bmatrix} \cos \theta_i \\ \sin \theta_i \end{bmatrix} = \begin{bmatrix} W \\ 0 \end{bmatrix}, \quad i = 1, 2, \dots, N_b, \quad (2)$$

where

$$\delta_i(x, y, t) = x \cos \theta_i + y \sin \theta_i - \delta_0,$$

$$\theta_i = 2\pi(i-1)/N_b + \omega_c t,$$

$$\omega_c = \omega r_i / (r_i + r_o),$$

and $G(\cdot)$ is a Heaviside function. Here,

$$G(\delta_i) = \begin{cases} \delta_i & \text{if } \delta_i \geq 0, \\ 0 & \text{if } \delta_i < 0. \end{cases}$$

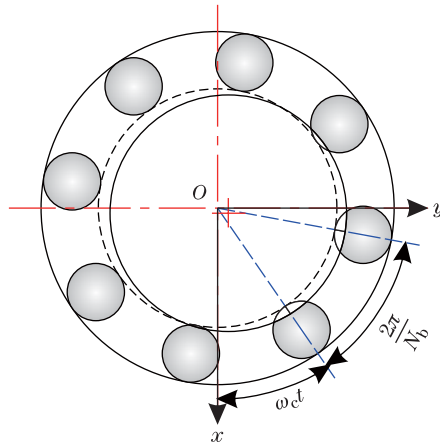


Fig. 1 Schematic diagram of ball bearing model

In the above equations, m is the mass of the rotor and the inner ring, C is the system damping, C_b is the Hertz contact stiffness between the balls and the inner-outer rings, δ_i is the i th small displacement between the i th ball and the bearing raceway, δ_0 is the radial clearance of the bearing, W is the weight supported by the outer ring, ω is the angular velocity of the rotor shaft, θ_i is the instant angular location of the i th ball, ω_c is the cage angular velocity, N_b is the number of balls, r_i and r_o are the radii of the inner and the outer rings, and $G(\cdot)$ takes \cdot and 0 representing the contact and non-contact cases between a ball and the outer ring, respectively.

According to the similarity theory^[30], define $\tau = \omega_c t$ and denote $(\cdot)'$ by differentiation with respect to τ . Then, Eq. (2) can be transformed into

$$\Omega^2 \begin{bmatrix} x'' \\ y'' \end{bmatrix} + \tilde{C}\Omega \begin{bmatrix} x' \\ y' \end{bmatrix} + \begin{bmatrix} f_x(x, y, \tau) \\ f_y(x, y, \tau) \end{bmatrix} = \begin{bmatrix} \tilde{W} \\ 0 \end{bmatrix}, \quad (3)$$

where

$$\begin{bmatrix} f_x(x, y, \tau) \\ f_y(x, y, \tau) \end{bmatrix} = \tilde{C}_b \sum_{i=1}^{N_b} G(\tilde{\delta}_i)^{\frac{1}{2}} \begin{bmatrix} \cos \tilde{\theta}_i \\ \sin \tilde{\theta}_i \end{bmatrix}. \quad (4)$$

Here,

$$\begin{aligned} \tilde{\delta}_i(x, y, \tau) &= x \cos \tilde{\theta}_i + y \sin \tilde{\theta}_i - \delta_0, \quad \tilde{\theta}_i = 2\pi(i-1)/N_b + \tau, \quad i = 1, 2, \dots, N_b, \\ \tilde{C}_b &= C_b/m, \quad \Omega = \omega_c, \quad \tilde{C} = C/m. \end{aligned}$$

From Eqs. (3) and (4), one can see the problem, dealt with in this article, is a parametrically excited system with the multiple piecewise $G(\tilde{\delta}_i)$, where $G(\tilde{\delta}_i)$ is also a complicated function. Therefore, the common analytical method is not available for this problem^[32].

3.2 HB-AFT scheme

Firstly, do the process of harmonic balance to Eq. (3).

The periodic solution forms of x and y can be represented as

$$\begin{bmatrix} x \\ y \end{bmatrix} = \begin{bmatrix} a_{x0} \\ a_{y0} \end{bmatrix} + \sum_{k=1}^K \left[\begin{bmatrix} a_{xk} \\ a_{yk} \end{bmatrix} \cos(k\tau) - \begin{bmatrix} b_{xk} \\ b_{yk} \end{bmatrix} \sin(k\tau) \right]. \quad (5)$$

The nonlinear restoring forces of $f_x(x, y, \tau)$ and $f_y(x, y, \tau)$ can be also written as

$$\begin{bmatrix} f_x \\ f_y \end{bmatrix} = \begin{bmatrix} c_{x0} \\ c_{y0} \end{bmatrix} + \sum_{k=1}^K \left[\begin{bmatrix} c_{xk} \\ c_{yk} \end{bmatrix} \cos(k\tau) - \begin{bmatrix} d_{xk} \\ d_{yk} \end{bmatrix} \sin(k\tau) \right]. \quad (6)$$

In Eqs. (5) and (6), K represents the maximum number of the considered harmonic terms.

Substituting Eqs. (5) and (6) into Eq. (3) and balancing the coefficients of each order harmonic, one can obtain the algebraic equations \mathbf{g} . For the constant terms,

$$\begin{bmatrix} \mathbf{g}(1) \\ \mathbf{g}(2) \end{bmatrix} = \begin{bmatrix} c_{x0} \\ c_{y0} \end{bmatrix} - \begin{bmatrix} \tilde{W} \\ 0 \end{bmatrix} = 0. \quad (7a)$$

For the cosine terms,

$$\begin{bmatrix} \mathbf{g}(4k-1) \\ \mathbf{g}(4k) \end{bmatrix} = k^2 \Omega^2 \begin{bmatrix} a_{xk} \\ a_{yk} \end{bmatrix} + k\Omega \tilde{C} \begin{bmatrix} b_{xk} \\ b_{yk} \end{bmatrix} - \begin{bmatrix} c_{xk} \\ c_{yk} \end{bmatrix}. \quad (7b)$$

For the sine terms,

$$\begin{bmatrix} \mathbf{g}(4k+1) \\ \mathbf{g}(4k+2) \end{bmatrix} = k\Omega\tilde{C} \begin{bmatrix} a_{xk} \\ a_{yk} \end{bmatrix} - k^2\Omega^2 \begin{bmatrix} b_{xk} \\ b_{yk} \end{bmatrix} + \begin{bmatrix} d_{xk} \\ d_{yk} \end{bmatrix}. \quad (7c)$$

In the above equations, $k = 1, 2, \dots, K$.

Let

$$\begin{bmatrix} \mathbf{P} \\ \mathbf{Q} \end{bmatrix}^T = \begin{bmatrix} a_{x0} & a_{y0} & a_{x1} & a_{y1} & b_{x1} & b_{y1} & \cdots & a_{xK} & a_{yK} & b_{xK} & b_{yK} \\ c_{x0} & c_{y0} & c_{x1} & c_{y1} & d_{x1} & d_{y1} & \cdots & c_{xK} & c_{yK} & d_{xK} & d_{yK} \end{bmatrix}^T, \quad (8)$$

where \mathbf{P} and \mathbf{Q} represent the coefficients of harmonics of displacements and nonlinear restore forces, respectively.

Take \mathbf{P} as an unknown variable. Using Eqs. (5)–(7), one can iterate to find the fix point \mathbf{P} . Here, the Newton-Raphson method is taken for the iteration, that is,

$$\mathbf{J}^{(i)}(\mathbf{P}^{(i+1)} - \mathbf{P}^{(i)}) + \mathbf{g}^{(i)}, \quad (9)$$

where \mathbf{J} is the Jacobian matrix, i.e., $\mathbf{J} = \frac{\partial \mathbf{g}}{\partial \mathbf{P}}$.

After the process of harmonic balance, the values of \mathbf{Q} and \mathbf{J} in each step of iterations can be obtained by the alternating frequency/time (AFT) technique.

For a supposed \mathbf{P} , an IDFT is first used to obtain discrete values of $x(\tau)$ and $y(\tau)$,

$$\begin{bmatrix} x(n) \\ y(n) \end{bmatrix} = \begin{bmatrix} a_{x0} \\ a_{y0} \end{bmatrix} + \sum_{k=1}^K \left[\begin{bmatrix} a_{xk} \\ a_{yk} \end{bmatrix} \cos \frac{2\pi kn}{N} - \begin{bmatrix} b_{xk} \\ b_{yk} \end{bmatrix} \sin \frac{2\pi kn}{N} \right], \quad (10)$$

where $n = 0, 1, \dots, N$. Here, $x(n)$ and $y(n)$ denote the sampled points at the n th discrete time, i.e., $x(n\Delta T)$ and $y(n\Delta T)$, where $\Delta T = 2\pi/N$, and N is the number of samples in the time domain.

According to Eqs. (4) and (10), the nonlinear restoring forces $f_x(x, y, \tau)$ and $f_y(x, y, \tau)$ can be discreted into

$$\begin{bmatrix} f_x(n) \\ f_y(n) \end{bmatrix} = \begin{bmatrix} f_x(x(n), y(n), 2\pi n/N) \\ f_y(x(n), y(n), 2\pi n/N) \end{bmatrix}. \quad (11)$$

The discrete values of $f_x(x, y, \tau)$ and $f_y(x, y, \tau)$ in the frequency domain can be obtained by the DFT as \mathbf{Q} , that is,

$$\begin{bmatrix} c_{x0} \\ c_{y0} \end{bmatrix} = \frac{1}{N} \sum_{n=0}^{N-1} \begin{bmatrix} f_x(n) \\ f_y(n) \end{bmatrix}, \quad (12a)$$

$$\begin{bmatrix} c_{xk} \\ c_{yk} \end{bmatrix} = \frac{2}{N} \sum_{n=0}^{N-1} \begin{bmatrix} f_x(n) \\ f_y(n) \end{bmatrix} \cos \frac{2\pi kn}{N}, \quad (12b)$$

$$\begin{bmatrix} d_{xk} \\ d_{yk} \end{bmatrix} = -\frac{2}{N} \sum_{n=0}^{N-1} \begin{bmatrix} f_x(n) \\ f_y(n) \end{bmatrix} \sin \frac{2\pi kn}{N}, \quad (12c)$$

where $k = 1, 2, \dots, K$.

According to Eq. (7) and Eqs. (10)–(12), the elements of \mathbf{J} in Eq. (9) can be deduced into

$$\left\{ \begin{aligned} \frac{\partial g(1)}{\partial p(1)} = \frac{\partial c_{x0}}{\partial a_{x0}} &= \frac{3}{2N} \tilde{C}_b \sum_{n=0}^{N-1} \sum_{i=1}^{N_b} G(\delta_i(n))^{0.5} \cos^2 \tilde{\theta}_{i,n}, \\ \frac{\partial g(1)}{\partial p(2)} = \frac{\partial c_{x0}}{\partial a_{y0}} &= \frac{3}{2N} \tilde{C}_b \sum_{n=0}^{N-1} \sum_{i=1}^{N_b} G(\delta_i(n))^{0.5} \sin \tilde{\theta}_{i,n} \cos \tilde{\theta}_{i,n}, \\ &\vdots \\ \frac{\partial g(4k+2)}{\partial p(4j+1)} = \frac{\partial d_{yk}}{\partial b_{xj}} &= \frac{3}{N} \tilde{C}_b \sum_{n=0}^{N-1} \sum_{i=1}^{N_b} (G(\delta_i(n))^{0.5} \sin \tilde{\theta}_{i,n} \cos \tilde{\theta}_{i,n}) \sin \frac{2\pi jn}{N} \sin \frac{2\pi kn}{N}, \\ \frac{\partial g(4k+2)}{\partial p(4j+2)} &= -k^2 \Omega^2 + \frac{\partial d_{yk}}{\partial b_{yj}} \\ &= -k^2 \Omega^2 + \frac{3}{N} \tilde{C}_b \sum_{n=0}^{N-1} \sum_{i=1}^{N_b} (G(\delta_i(n))^{0.5} \cos^2 \tilde{\theta}_{i,n}) \sin \frac{2\pi jn}{N} \sin \frac{2\pi kn}{N}, \end{aligned} \right. \quad (13)$$

where

$$\begin{aligned} k, j &= 1, 2, \dots, K, \quad \tilde{\delta}_i(n) = x(n) \cos \tilde{\theta}_{i,n} + y(n) \sin \tilde{\theta}_{i,n} - \delta_0, \\ \tilde{\theta}_{i,n} &= \frac{2\pi(i-1)}{N_b} + \frac{2\pi n}{N}. \end{aligned}$$

By combining the process of harmonic balance and AFT, the iterations of Eq. (9) can readily yield \mathbf{P} in proper accuracy. The procedure is as follows:

- (i) For a supposed $\mathbf{P}^{(0)}$, obtain $\mathbf{Q}^{(0)}$ and $\mathbf{J}^{(0)}$ by using Eqs. (10), (12), and (13).
- (ii) Iterate Eq. (9) once, and get $\mathbf{P}^{(1)}$.
- (iii) Continue (i) and (ii) until the norm of $\mathbf{P}^{(m)} - \mathbf{P}^{(m-1)}$ is less than an allowed ε .

3.3 Stability analysis

In order to make a systematic study on the bifurcation characteristics of the system, one needs to analyze the stability of the periodic solutions obtained by the HB-AFT. In this study, the Floquet theory is employed^[17,20,25], and the method developed by Hsu is applied for approximating the monodromy matrix. Here, from the characteristics of the HB-AFT, a simplified strategy on the base of Hsu’s method can be proposed^[33].

Let

$$U = [x \quad x' \quad y \quad y']^T = [x_1 \quad x_2 \quad x_3 \quad x_4]^T.$$

Then, Eq. (3) can be transformed into

$$U'(\tau) = \begin{bmatrix} x_2 \\ (\tilde{W} - f_x(x_1, x_3, \tau))/\Omega^2 - \tilde{C}x_2/\Omega \\ x_4 \\ -f_y(x_1, x_3, \tau)/\Omega^2 - \tilde{C}x_4/\Omega \end{bmatrix} = F(\tau, U(\tau)). \quad (14)$$

Define $A(\tau, U(\tau))$ as

$$A(\tau, U(\tau)) = \frac{\partial F}{\partial U} = \begin{bmatrix} 0 & 1 & 0 & 0 \\ A_{21} & A_{22} & A_{23} & 0 \\ 0 & 0 & 0 & 1 \\ A_{41} & 0 & A_{43} & A_{44} \end{bmatrix}, \quad (15)$$

where

$$\begin{aligned} A_{22} &= A_{44} = \tilde{C}/\Omega, \\ A_{21} &= -\frac{3\tilde{C}_b}{2\Omega^2} \sum_{i=1}^{N_b} G(\delta_i(n))^{0.5} \cos^2 \tilde{\theta}_i, \\ A_{43} &= -\frac{3\tilde{C}_b}{2\Omega^2} \sum_{i=1}^{N_b} G(\delta_i(n))^{0.5} \sin^2 \tilde{\theta}_i, \\ A_{23} &= A_{41} = -\frac{3\tilde{C}_b}{2\Omega^2} \sum_{i=1}^{N_b} G(\delta_i(n))^{0.5} \sin \tilde{\theta}_i \cos \tilde{\theta}_i. \end{aligned}$$

For the system of Eq. (14), give ΔU to perturb the assumed equilibrium U^* and have

$$\Delta U' = F(\tau, U^* + \Delta U). \quad (16)$$

Then, the stability of U^* can be obtained by the linear stability of ΔU in the following system:

$$\Delta U' = \frac{\partial F(\tau, U^*)}{\partial U^*} \Delta U = A(\tau, U^*(\tau)) \Delta U. \quad (17)$$

According to Hsu's method, the approximating monodromy matrix can be expressed as^[22]

$$M = \Psi(T) = \prod_{\bar{n}=\bar{N}}^1 \exp(A_{\bar{n}} \Delta T) = \prod_{\bar{n}=\bar{N}}^1 \left(I + \sum_{j=1}^{n_j} \frac{(A_{\bar{n}} \Delta T)^j}{j!} \right). \quad (18)$$

Here, I denotes the identity matrix, and a constant matrix $A_{\bar{n}}$ substitutes the time-varying matrix $A(\tau, U(\tau))$ in the \bar{n} th time interval, that is,

$$A_{\bar{n}} = \frac{1}{\Delta T} \int_{\tau_{\bar{n}-1}}^{\tau_{\bar{n}}} A(\tau, U^*(\tau)) d\tau, \quad (19)$$

where

$$\tau_{\bar{n}} = \bar{n} \Delta T / \bar{N}, \quad \bar{n} = 1, 2, \dots, \bar{N}.$$

Combining the HB-AFT process, we get

$$A_{\bar{n}} \approx A(\tau_{\bar{n}}, U^*(\tau_{\bar{n}})). \quad (20)$$

The substitution has been done for two reasons. First, some of the systems have complicated equation forms. Taking Eq. (20) rather than Eq. (19) can avoid the difficulties of complicated integrations. For instance, the problem of Eq. (15) studied here has multiple piecewise irrational functions of $G(\delta_i(n))^{0.5}$, where $i = 1, 2, \dots, N_b$. These functions are very hard to integrate. Second, this simplification can maintain internal consistency of discretization of the HB-AFT scheme. The elements of $A(\tau, U(\tau))$ are components of the elements of the Jacobian matrix elements (see Eq. (13)), which can reduce the work of the programming calculation.

4 Results and discussion

The rotor bearing system under analysis is shown in Eq. (3). The reference values in the equation are from Ref. [8] as follows:

$$\begin{aligned} N_b &= 9, \quad \delta_0 = 2 \times 10^{-5} \text{ m}, \quad C_b = 7.055 \times 10^9 \text{ N/m}^{3/2}, \\ m &= 0.6 \text{ kg}, \quad W = 6 \text{ N}, \quad C = 200 \text{ N} \cdot \text{s/m}. \end{aligned}$$

From Eq. (3), one can see that the studied model is a parametrical excited system, and $T = 2\pi/\Omega$ is the excited period, where Ω is the revolution angular velocity of the balls. When $K = 36$ (in Eq. (5)), $N = 144$ (in Eq. (10)), $\varepsilon = 10^{-19}$, and $\Omega = 500$ rad/s, the analytical approximation of the period-1 solution obtained by the HB-AFT method is (here, the harmonic terms, whose coefficients are less than 10^{-18} , are not presented)

$$\begin{aligned} x(t) = & 2.102\,506\,128\,4 \times 10^{-5} \\ & + 6.845\,418\,049\,7 \times 10^{-7} \cos(\Omega_{vc}t) \\ & - 5.301\,357\,462\,4 \times 10^{-8} \sin(\Omega_{vc}t) \\ & + 4.593\,165\,428\,9 \times 10^{-8} \cos(2\Omega_{vc}t) \\ & - 3.850\,990\,157\,2 \times 10^{-9} \sin(2\Omega_{vc}t) \\ & - 2.347\,191\,184\,2 \times 10^{-9} \cos(3\Omega_{vc}t) \\ & - 5.821\,683\,258\,2 \times 10^{-10} \sin(3\Omega_{vc}t) \\ & - 7.833\,122\,168\,1 \times 10^{-11} \cos(4\Omega_{vc}t) \\ & + 1.277\,043\,417\,1 \times 10^{-10} \sin(4\Omega_{vc}t), \end{aligned}$$

where $\Omega_{vc} = N_b\Omega$. The above expression of $x(t)$ suggests that the period-1 motion of the system is affected by the ball passage vibrations. Actually, the minimum period of the motion is T_{vc} rather than T , where $T_{vc} = 2\pi/\Omega_{vc}$. Here, $f_{vc} = 1/T_{vc}$ is usually called the varying compliance frequency [16].

As shown in Fig. 2, the HB-AFT results agree well with the numerical solutions of the fourth-order R-K method. The calculation of the HB-AFT has a fast convergence and a large convergent region, which can be seen in Fig. 3. In Fig. 3, the HB-AFT with initial iterative values of $\mathbf{P}^{(0)} = [0]$ except $\mathbf{P}^{(0)}(1) = 1.0$ via the 5th iteration has arrived at a solution close to the R-K integration corresponding to the round markers.

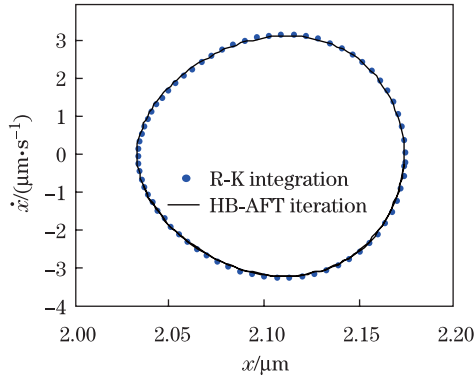


Fig. 2 Phase portrait of period-1 solution when $\Omega = 500$ rad/s

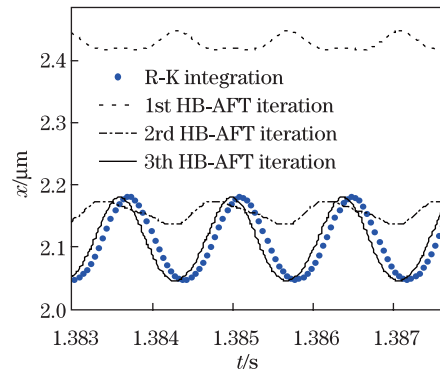


Fig. 3 Convergence of HB-AFT results under increasing iteration times

In order to analyze system's global periodic characteristics, taking Ω as a control parameter, using the HB-AFT method, search the period-1 solutions between 480 rad/s and 1000 rad/s with a step-size of 10 rad/s. By the simplified method shown in Section 3.3, the stability of the obtained solutions of period-1 is analyzed by the Floquet theory. It is found that the Floquet

multipliers keep a convergent accuracy to 0.01 with $\bar{N} = 2 \times 10^4$ and $n_j = 5$ (in Eq. (18)). Calculations show that the leading multipliers are inside the unit circle at $\Omega = 480$ rad/s to 690 rad/s, and the corresponding period-1 solutions are stable. From 700 rad/s to 950 rad/s, the leading multipliers are less than -1 . Hence, the corresponding period-1 solutions are unstable. Until $\Omega = 960$ rad/s, the leading multipliers come back to the unit circle from the negative real axis. Table 1 further indicates that the period doubling bifurcations occur in the angular velocity ranges of Ω from 697 rad/s to 698 rad/s and from 953 rad/s to 954 rad/s, which is basically consistent with the numerical result shown in Fig. 4.

Table 1 Leading multipliers of period-1 solutions in velocity range of period-doubling bifurcation developing

$\Omega/(\text{rad}\cdot\text{s}^{-1})$	696	697	698	699	952	953	954	955
Leading multipliers	-0.841	-0.943	-1.048	-1.156	-1.167	-1.080	-0.993	-0.906

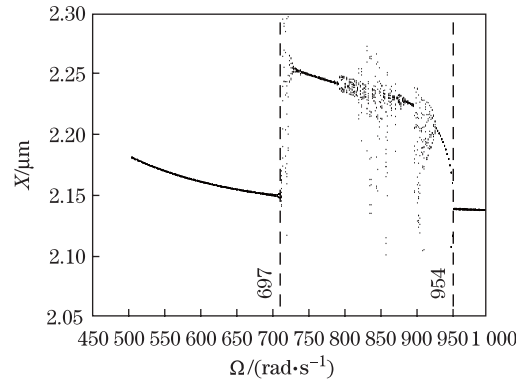


Fig. 4 Bifurcation diagrams versus parameter Ω and bifurcation locations of period-1 motion obtained by HB-AFT with Floquet theory

Note the fact that the period doubling bifurcation induces the instability of period-1 motion. Hence, in order to do deep investigation for dynamical behaviors of the system, it is necessary to analyze the response of period-2 motion in the range from 700 rad/s to 950 rad/s, which is unstable for period-1 motion. For example, when $K = 36$, $N = 144$, $\varepsilon = 10^{-19}$, and $\Omega = 930$ rad/s, the analytical approximation of the period-2 solution obtained by the HB-AFT method is (here the harmonic terms, whose coefficients are less than 10^{-18} , are not presented)

$$\begin{aligned}
 x(t) = & 2.116\ 112\ 472\ 8 \times 10^{-5} \\
 & - 7.233\ 511\ 078\ 2 \times 10^{-7} \cos\left(\frac{1}{2}\Omega_{\text{vct}}\right) \\
 & + 1.002\ 821\ 189\ 9 \times 10^{-7} \sin\left(\frac{1}{2}\Omega_{\text{vct}}\right) \\
 & + 1.403\ 582\ 154\ 0 \times 10^{-7} \cos(\Omega_{\text{vct}}) \\
 & - 5.503\ 670\ 942\ 4 \times 10^{-9} \sin(\Omega_{\text{vct}}) \\
 & - 1.361\ 807\ 888\ 1 \times 10^{-8} \cos\left(\frac{3}{2}\Omega_{\text{vct}}\right)
 \end{aligned}$$

$$\begin{aligned}
& + 3.888\,988\,506\,2 \times 10^{-9} \sin\left(\frac{3}{2}\Omega_{vc}t\right) \\
& - 8.183\,985\,232\,5 \times 10^{-10} \cos(2\Omega_{vc}t) \\
& + 2.697\,575\,219\,3 \times 10^{-11} \sin(2\Omega_{vc}t), \\
y(t) = & 1.849\,316\,343\,4 \times 10^{-7} \\
& + 2.140\,536\,071\,2 \times 10^{-9} \cos\left(\frac{1}{2}\Omega_{vc}t\right) \\
& - 5.800\,466\,765\,8 \times 10^{-8} \sin\left(\frac{1}{2}\Omega_{vc}t\right) \\
& + 1.000\,975\,497\,7 \times 10^{-9} \cos(\Omega_{vc}t) \\
& + 2.454\,074\,292\,3 \times 10^{-8} \sin(\Omega_{vc}t) \\
& - 9.131\,516\,590\,8 \times 10^{-10} \cos\left(\frac{3}{2}\Omega_{vc}t\right) \\
& - 5.546\,233\,711\,3 \times 10^{-9} \sin\left(\frac{3}{2}\Omega_{vc}t\right) \\
& + 1.161\,585\,592\,0 \times 10^{-11} \cos(2\Omega_{vc}t) \\
& + 1.195\,165\,426\,6 \times 10^{-9} \sin(2\Omega_{vc}t).
\end{aligned}$$

The result is close to the numerical simulation (see Fig. 5(a)), and this indicates that the system has period-2 motion at $\Omega = 930$ rad/s. As displayed in the above expressions of $x(t)$ and $y(t)$, the period-2 motion of the system is also affected by the ball passage vibrations. Actually, the minimum period of the motion is $2T_{vc}$ rather than T , which coincides with the power spectra shown by Fig. 5(b).

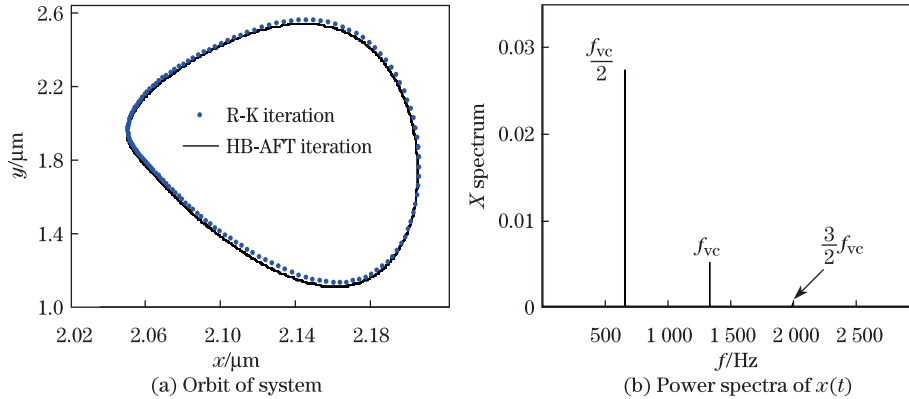


Fig. 5 Orbit of system and power spectra of $x(t)$ with $\Omega = 930$ rad/s

Using the present method, we continue to investigate the stability of the global period-2 motion of the system. The analysis indicates that the dynamical characteristics of period-2 motion are also interval stability, and the period doubling bifurcation is also a way to instability. However, Table 2 presents the case that two complex conjugate Floquet multipliers leave the unit circle, which indicates that the Neimark bifurcation^[11,25] occurs from $\Omega = 925$ rad/s to

928 rad/s. Figure 6 shows that the Poincaré maps are built by the R-K method at $\Omega = 926$ rad/s, 927 rad/s, and 928 rad/s. It is clear that the motion changes from quasi-periodic to periodic gradually, which is a strong evidence for the Neimark bifurcation in the period-2 motion.

Table 2 Leading multipliers of period-2 solutions in velocity range of Neimark bifurcation developing

$\Omega/(\text{rad}\cdot\text{s}^{-1})$	925	926	927	928
Leading multipliers	$-0.341 + 1.041i$	$-0.218 + 1.000i$	$-0.107 + 0.944i$	$-0.010 + 0.876i$

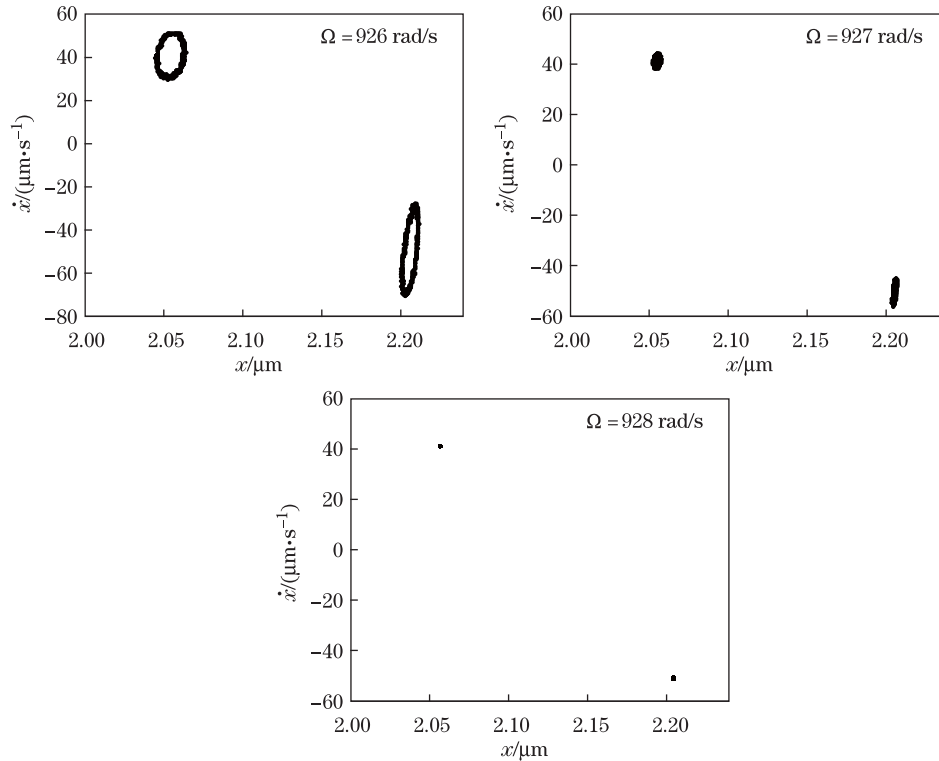


Fig. 6 Poincaré maps of $x(t)$ at 926 rad/s, 927 rad/s, and 928 rad/s

Figure 7(a) presents the global peak value characteristics of the period-1 and period-2 solutions by Ω as the horizontal axis. The peak of $x(t)$ is calculated by the HB-AFT as a function, where the square markers and the round markers correspond to the solutions to period-1 and period-2, respectively. In Fig. 7(a), the area of $A-A$ denotes the unstable velocity range of period-1 motion, and the three darker areas, i.e., $B-B$, $C-C$, and $D-D$, signify the unstable velocity ranges of period-1 and period-2 simultaneously. In these three areas, one can predict that the forms of motion are more complicated, and the chaotic motion may occur. The rotor bearing system would avoid working in these ranges. In fact, the largest Lyapunov exponent curve in Fig. 7(b) clearly indicates that the chaotic motion exists in the ranges of $B-B$, $C-C$, and $D-D$. Figure 8 affirms the existence of chaos in these ranges to be right further. It can be seen that the above process is an effective way to estimate the dangerous ranges of the system's motion.

5 Conclusions

Compared with other common methods, the HB-AFT method requires fewer analysis, especially the studies of integration and series expansion, during the solving processes. Thus,

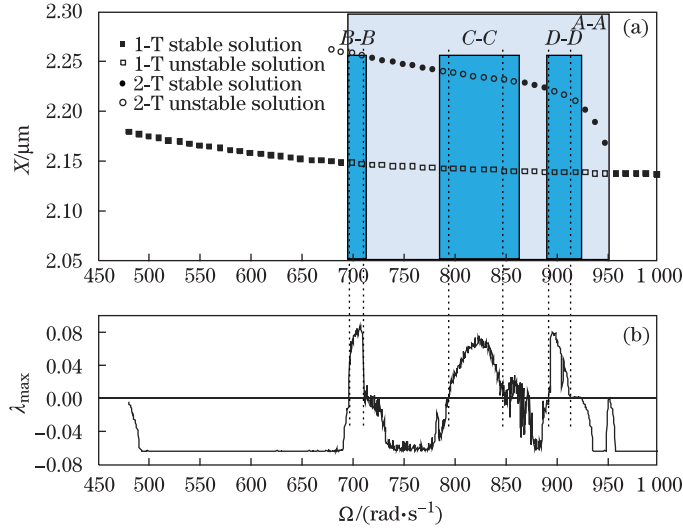


Fig. 7 Peak diagrams of global period-1 solution and period-2 solution, obtained by HB-AFT and largest Lyapunov exponent curve calculated by Wolf method^[34]

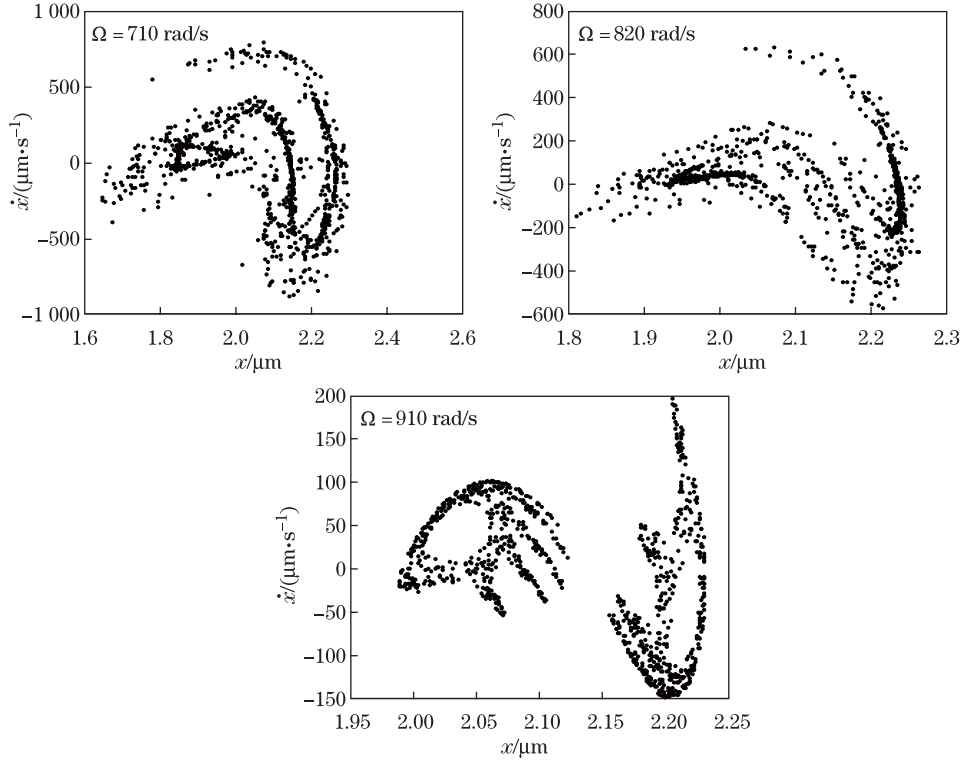


Fig. 8 Poincaré maps of $x(t)$ response at 710 rad/s, 820 rad/s, and 910 rad/s

this method is well-suited for the fractional exponential problems, even the problem with piecewise-irrational nonlinearities. It is also an efficient method because of its property of fast convergence in a large range.

Using the HB-AFT method, a rigid rotor-ball-bearing system is analyzed. The analysis indicates that the dynamical characteristics of periodic motion are interval stability, and the period doubling bifurcation and the Neimark bifurcation are two ways to instability for the system.

Besides, combining the treatment of the HB-AFT method, a simplified strategy to determine the Floquet multipliers is proposed. A way to give a fast estimation of the dangerous motion range is presented, which may be significant for the global response analysis and the dynamic optimal design of the nonlinear systems.

Acknowledgements We gratefully acknowledge Professor A. C. J. LUO for many valuable suggestions to this work during his seminars in Harbin, China.

References

- [1] Jin, D. P., Hu, H. Y., and Wu, Z. Q. Analysis of vibro-impacting flexible beams based on Hertzian contact model (in Chinese). *Journal of Vibration Engineering*, **11**(1), 46–51 (1998)
- [2] Yigit, A. S., Ulsoy, A. G., and Scott, R. A. Spring-dashpot models for the dynamics of a radically rotating beam with impact. *Journal of Sound and Vibration*, **142**(3), 515–525 (1990)
- [3] Yamauchi, S. The nonlinear vibration of flexible rotors. *Transaction of JSME, Series C*, **446**, 1862–1868 (1983)
- [4] Kim, Y. B. and Noah, S. T. Stability and bifurcation analysis of oscillators with piecewise-linear characteristics: a general approach. *ASME Journal of Applied Mechanics*, **58**(2), 545–553 (1991)
- [5] Kim, Y. B. and Noah, S. T. Response and bifurcation analysis of an MDOF rotor system with a strong nonlinearity. *Nonlinear Dynamics*, **2**, 215–234 (1991)
- [6] Kim, Y. B. and Noah, S. T. Quasi-periodic response and stability analysis for a non-linear Jeffcott rotor. *Journal of Sound and Vibration*, **190**(2), 239–253 (1996)
- [7] Groll, G. V. and Ewins, D. J. The harmonic balance method with arc-length continuation in rotor/stator contact problems. *Journal of Sound and Vibration*, **241**(2), 223–233 (2001)
- [8] Tiwari, M. and Gupta, K. Effect of radial internal clearance of a ball bearing on the dynamics of a balanced horizontal rotor. *Journal of Sound and Vibration*, **238**(5), 723–756 (2000)
- [9] Villa, C., Sinou, J. J., and Thouverez, F. Stability and vibration analysis of a complex flexible rotor bearing system. *Communications in Nonlinear Science and Numerical Simulation*, **13**, 804–821 (2008)
- [10] Cash, J. R. and Karp, A. H. A variable order Runge-Kutta method for initial value problems with rapidly varying right-hand sides. *ACM Transactions on Mathematical Software*, **16**(3), 201–222 (1990)
- [11] Nayfeh, A. H. and Balachandran, B. *Applied Nonlinear Dynamics*, Wiley InterScience, New York (1995)
- [12] Ling, F. H. A numerical treatment of the periodic solutions of non-linear vibration systems. *Applied Mathematics and Mechanics (English Edition)*, **4**(4), 525–546 (1983) DOI 10.1007/BF01874666
- [13] Hu, H. Y. Numerical scheme of locating the periodic response of non-smooth non-autonomous systems of high dimension. *Computer Methods in Applied Mechanics and Engineering*, **123**(1), 53–62 (1995)
- [14] Li, D. X. and Xu, J. X. Periodic solution and its approximate analytic expressions of the nonlinear rotor bearing system (in Chinese). *Chinese Journal of Computational Mechanics*, **21**(5), 557–563 (2004)
- [15] Choi, S. K. and Noah, S. T. Response and stability analysis of piecewise-linear oscillators under multi-forcing frequencies. *Nonlinear Dynamics*, **3**, 105–121 (1992)

-
- [16] Bai, C. Q., Xu, Q. Y., and Zhang, X. L. Nonlinear stability of balanced rotor due to effect of ball bearing internal clearance. *Applied Mathematics and Mechanics (English Edition)*, **27**(2), 175–186 (2006) DOI 10.1007/s10483-006-0205-1
- [17] Zhou, J. Q. and Zhu, Y. Y. *Nonlinear Vibrations* (in Chinese), Xi'an Jiao Tong University Press, Xi'an (1998)
- [18] Press, W. H., Teukolsky, S. A., Vetterling, W. T., and Flannery, B. P. *Numerical Recipes in Fortran the Art of Scientific Computing*, 2nd ed., Cambridge University Press, Cambridge (1992)
- [19] Chua, L. O. and Akio, U. Algorithms for computing almost periodic steady state response of nonlinear systems to multiple input frequencies. *IEEE Transactions on Circuits and Systems*, **28**, 953–971 (1981)
- [20] Chen, Y. S. *Nonlinear Vibrations* (in Chinese), Higher Education Press, Beijing (2002)
- [21] Lau, S. L. and Cheung, Y. K. Amplitude incremental variational principle for nonlinear vibration of elastic systems. *ASME Journal of Applied Mechanics*, **48**, 959–964 (1981)
- [22] Shen, J. H., Lin, K. C., Chen, S. H., and Sze, K. Y. Bifurcation and route-to-chaos analyses for Mathieu-Duffing oscillator by the incremental harmonic balance method. *Nonlinear Dynamics*, **52**, 403–414 (2008)
- [23] Aghothama, A. R. and Arayanan, S. N. Bifurcation and chaos in geared rotor bearing system by incremental harmonic balance method. *Journal of Sound and Vibration*, **226**(3), 469–492 (1999)
- [24] Yang, S. P. and Shen, Y. J. Nonlinear dynamics of gear system based on incremental harmonic balance method (in Chinese). *Journal of Vibration and Shock*, **24**(3), 40–42 (2005)
- [25] Hu, H. Y. *Applied Nonlinear Dynamics* (in Chinese), Aviation Industry Press, Beijing (2000)
- [26] Zorich, V. A. *Mathematical Analysis II*, Springer, Berlin (2002)
- [27] Cameron, T. M. and Griffin, J. H. An alternating frequency/time domain method for calculating the steady state response of nonlinear dynamic systems. *ASME Journal of Applied Mechanics*, **56**, 149–154 (1989)
- [28] Luo, A. C. J. *Continuous Dynamical Systems*, Higher Education Press, Beijing (2012)
- [29] Luo, A. C. J. *Regularity and Complexity in Dynamical Systems*, Springer-Verlage, New York (2012)
- [30] Arnold, V. I. *Mathematical Methods of Classical Mechanics*, 2nd ed., Springer-Verlag, New York (1991)
- [31] Liew, A., Feng, N., and Hahn, E. J. Transient rotordynamic modeling of rolling element bearing systems. *Journal of Engineering for Gas Turbines and Power*, **124**, 984–991 (2002)
- [32] Gao, S. H., Long, X. H., and Meng, G. Nonlinear response and nonsmooth bifurcations of an unbalanced machine-tool spindle-bearing system. *Nonlinear Dynamics*, **54**, 365–377 (2008)
- [33] Friedmann, P. and Hammond, C. E. Efficient numerical treatment of periodic systems with application to stability problems. *International Journal for Numerical Methods in Engineering*, **11**, 1117–1136 (1977)
- [34] Wolf, A., Swift, J. B., Swinney, H. L., and Vastano, J. A. Determining Lyapunov exponents from a time series. *Physica D*, **16**, 285–317 (1985)